ISSN: 2639-7455

Research Article

Earth & Environmental Science Research & Reviews

Shelf Currents within Different Oceans Under the Sun-Moon Gravitation

Zhiren Wang

Institute of Marine and Coastal Sciences, Rutgers, The State University of New Jersey

***Corresponding author**
Zhiren Wang, Institute of Marine and Coastal Sciences, Rutgers, The State University of New Jersey, 71 Dudley Road, New Brunswick, NJ 08901; Email: joewwh77@gmail.com

Submitted: 10 Jan 2019; **Accepted**: 17 Jan 2019; **Published**: 20 Feb 2019

Abstract

Here, I employed the shelf properties and sizes of different basins and introduced the Sun-Moon gravitation into the dynamical equations to dynamically explain the differences existing in the Gulf Stream and the Kuroshio systems. In addition to the classic western-boundary intensification of the western boundary currents that fails to explain why the differences in currents and ENSO significance exist among different oceans, shelf properties and sizes of different basins may produce another western-boundary intensification of the western boundary currents under the Sun-Moon gravitation.

Introduction

As important western boundary currents (WBC), the Gulf Stream in the North Atlantic and the Kuroshio in the North Pacific play important roles interaction between dynamics and thermodynamics and between the atmosphere and oceans [1-6]. The substantial similarities in the Gulf Stream and the Kuroshio systems, such as geostrophic advection, anti-correlation between path stability and surface transport, and similar effects on SST, might be associated with western-boundary intensification of the WBC [7].

However, the classic western-boundary intensification of the WBC cannot explain the differences existing in the Gulf Stream and the Kuroshio systems, e.g., for their response to large-scale winds, and cannot explain why there is no similar WBC in Indian Ocean. The differences in WBC may be related to the characteristic (sizes and shelf slopes) of the basins [7].

Basin sizes can make difference in currents. The zonal wave oscillation intensity of the Sun-Moon gravitation (SMG), expressed as the zonal contrast of the mean SMG within a basin, are different and can cause differences in the zonal oscillation intensity in different oceans. SMG wave covers one to two waves along the entire latitude parallels. In the Pacific Ocean whose zonal size covers approximately 0.5-1.0 wavelengths of the one to two SMG waves, the zonal oscillation intensity is 1.5-2 times that of the Atlantic and Indian Oceans whose zonal sizes are much shorter than the SMG wavelengths. The strongest zonal oscillation intensity likely makes the ENSO most prominent in the Pacific Ocean.

The shelf properties (e.g., slope) of basins may also change currents. The shelf currents on the continental shelves of the three oceans were estimated by introducing the SMG into the dynamical shallow water equations. In addition to the vorticity source from Coriolis force, the SMG is the major vorticity source for the whole depth of tropical oceans, approximately 2 to 4 times of that provided by wind stress. Related to the Earth's radius (Re), thickness (H) of water column, and shelf's slope (Sx), the SMG-induced shelf currents can be amplified by HSx-1Re-1 times due to the shelf's slope, with the large and slow west shelf of the Pacific Ocean intensifying the flows on it much more than the small and sharp west shelves of the Indian and the Atlantic Oceans.

The difference in the size and slope among the western shelves of the Indian, Pacific, and Atlantic Oceans is significant and makes difference in producing western boundary flows. The amplified flows on the western shelf of the Pacific Ocean is a new "western intensification" and contribute to the fact that the ENSO oscillation is the most significant in the Pacific Ocean among the three oceanic basins.

Governor equations and the major flow vorticity source

Here the continental shelf is defined as the slope oceanic bottom from seashore till the base of basin. Through applying the dynamical shallow water equations for the water under the SMG, the momentum equations can be written as [8].

$$\frac{\partial u}{\partial t}+u\frac{\partial u}{\partial x}+v\frac{\partial u}{\partial y}-fv=-g\frac{\partial h}{\partial x}+\sum_{i=M}^{S}g_{ix}+\frac{\tau_x}{\rho(h+H)}-\epsilon(t)u \quad (1)$$

$$\frac{\partial v}{\partial t}+u\frac{\partial v}{\partial x}+v\frac{\partial v}{\partial y}+fu=-g\frac{\partial h}{\partial y}+\sum_{i=M}^{S}g_{iy}+\frac{\tau_y}{\rho(h+H)}-\epsilon(t)v \quad (2)$$

$$\frac{\partial H}{\partial t}+u\frac{\partial H}{\partial x}+v\frac{\partial H}{\partial y}+H\left(\frac{\partial u}{\partial x}+\frac{\partial v}{\partial y}\right)=-\epsilon(t)H \quad (3)$$

where, $\{u, v\} = \{u, v\}\{x, y, t\}$ are whole-depth mean zonal and meridional flow speeds, respectively; t_x and t_y are wind stress in zonal and meridional directions, respectively; $h\{x, y, t\}$ and $H\{x, y t\}$ are the heights of free surface and the mean thickness of entire water column, respectively; $f = 2f_e sin\varphi$, $p \approx 1010 kgm^{-3}$, the density of sea water; ϵ is Rayleigh dissipation coefficient, depending on the length of time scale T_{sc}. With $t \to \infty$, $\epsilon \propto \lim_{n \to \infty} T_{sc}^{-1}$, and

$$g_{ix} = -g_{io}(k_i sin\varphi \sin t_r \sin\ t_f\ + 0.5 cos\varphi sin2t_f) \quad (4)$$

$$g_{iy} = g_{io}[0.5 sin2\varphi(k_i^2 sin^2\ t_r - cos^2\ t_f)\ + k_i cos2\varphi cost_f \sin t_r] \quad (5)$$

$$t_f = t(f_e - f_{ir}) + \lambda_{ic} \quad (6)$$

$$t_r = f_{ir}(t + t_i) \quad (7)$$

The vorticity equation is derived from Eq. 1, 2 and 3, as

$$\frac{d}{dt}\frac{V_{or}}{H} = \frac{1}{H}[\epsilon(t)f + \frac{\partial}{\partial x}\frac{\tau_y}{\rho(h+H)} - \frac{\partial}{\partial y}\frac{\tau_x}{\rho(h+H)}] +$$

$$\frac{1}{R_e H} sin\varphi \sum_{i=M}^{S} g_{io}[\lambda_{ic} cos2t_f + \frac{1}{2} sin2t_f$$

$$+ k_i sin(f_{ir}t) tg\varphi(\lambda_{ic} cost_f + sint_f)] \quad (8)$$

where, vorticity

$$V_{or} = f + \frac{\partial v}{\partial x} - \frac{\partial u}{\partial y}, \text{ and } \frac{d}{dt} = \frac{\partial}{\partial t} + u\frac{\partial}{\partial x} + v\frac{\partial}{\partial y}.$$

Integrating Eq. 8 along time (t) and averaging Eq.8 within entire depth (H) of the water column by making $\frac{1}{H}\int_0^H \int \{\text{Eq.8}\}\ \text{dtdz}$

and considering fe >> |*u*, *v*|/ R_e

$$\frac{\partial V}{\partial x} - \frac{\partial U}{\partial y} = \int[\frac{\partial}{\partial x}\frac{\tau_y}{\rho(h+H)} - \frac{\partial}{\partial y}\frac{\tau_x}{\rho(h+H)}]dt + \sum_{i=M}^{S} g_{io} F_i(x,y,t)$$

$$+ C_o H + 2f_e sin\varphi[\int \epsilon(t)dt - 1] \quad (9)$$

where, C_o is an integrating constant,

$$F_i = \int \frac{sin\varphi}{R_e H}[\lambda_{ic} cos2t_f + \frac{1}{2} sin2t_f +$$

$$k_i sin(f_{ir}t) tg\varphi(\lambda_{ic} cost_f + sint_f)]dt$$

$$= \frac{sin\varphi}{4 f_e R_e}[2q_{2H} + cos2t_f + 4C_i(q_{1H} + cost_f)] \quad (10)$$

$$U = \frac{1}{H}\int_0^H udz \quad (11)$$

$$V = \frac{1}{H}\int_0^H vdz \quad (12)$$

$$q_{nH} = a_H \sin(nt_f)\, CosInt(na_H) + a_H \cos(nt_f)\, SinInt(na_H) \quad (13)$$

(n=1 or 2)

$$a_H = \frac{H}{S_x R_e cos\varphi} \quad (14)$$

$$C_i = k_i tg\varphi \sin(f_{ir}t) \quad (15)$$

The daily Quick Scat winds of year 2006 are applied here for computation of the averaged absolute values of the wind stress-generation term (the first two terms in the right hand side of Eq. 9) and the SMG-generation term (the third term in the right hand side of Eq. 9). As far as averaged within the entire depth of tropical oceans and within a whole year is concerned, the mean size of vorticity source provided by the SMG is about 2 to 4 times of that provided by wind stress (Fig. 1).

Except the vorticity sources from Coriolis force, topography, and dissipation (the last three terms in the right hand side of Eq. 9), the SMG is the major vorticity source for the whole depth of tropical oceans. Both the SMG-generation term and wind stress-generation term make no significant difference among different oceanic basins.

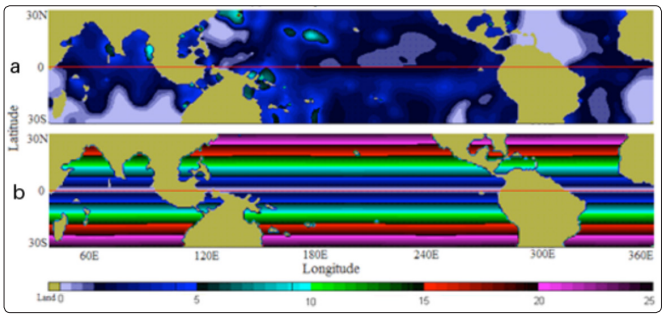

Figure 1: The mean size of vorticity source ($\times 10^{-14}$ s^{-2}) provided by wind stress (**a**) and by the SMG (**b**), computed from daily Quick Scat wind and SMG during 2006 by using Eq. 9 and 10

Solution of the flows on the shelves under the SMG

The contribution of the SMG to currents on the western continental shelf of the three tropical oceans is estimated for regions: $x \in [x_w, x_e]$ and $y \in [y_s, y_n]$. The x_w, x_e, y_s,and y_n are the coordinates of the west, east, south, and north boundaries for the continental shelf of the three tropical oceans. Each subdivision is a zonal belt that is narrow, and the continental shelf within each subdivision is approximated as a plane that has only a longitudinal slope, i.e., the mean slope plane from seashore till the base of basin (Fig.2).

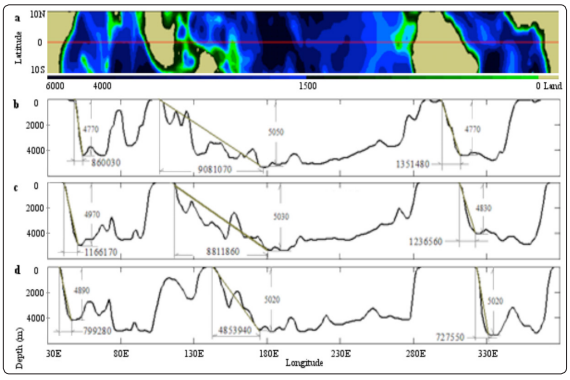

Figure 2: Topography (m) of oceans (a) and their depths (m) averaged within 6°N − 10°N (b), 2°S − 2°N (c), and 6°S − 10°S (d). The brown thick lines represent the mean slope from seashore to the base of basins

The depth of the water column within each subdivision only change with x, as

$$H = H_w + xS_x \quad (16)$$

The slope of the continental shelf is,

$$S_x = \frac{H_o - H_w}{x_e - x_w} \quad (17)$$

$$H_w = H(x = x_w) \quad (18)$$

$$H_o = H(x = x_e) \quad (19)$$

Using Eq. 16, the mass-conservation equation 3 is accordingly simplified as,

$$\frac{\partial u}{\partial x} + \frac{\partial v}{\partial y} = -\frac{u}{H}S_x - \epsilon(t)$$

After averaged within entire depth,

$$\frac{\partial U}{\partial x} + \frac{\partial V}{\partial y} = -\frac{U}{H}S_x - \epsilon \quad (20)$$

Within the narrow tropical zonal belts with $y_n - y_s = 4°$, $y/R_e = \varphi_m \approx$ const, $\frac{\partial^2 U}{\partial y^2} \approx 0$, omitting wind stress and topography terms, and combing Eq. 9 and Eq. 20 to cancel V,

$$\left(\frac{\partial^2}{\partial x^2} + \frac{S_x}{H}\frac{\partial}{\partial x} - \frac{S_x^2}{H}\right) U = \frac{2C_k f_e}{R_e} cos\varphi_m + \frac{1}{f_e R_e}\sum_{i=M}^{S} g_{io}\frac{\partial}{\partial y}F_i \quad (21)$$

Where, $0 < C_k = 1 - \int \varepsilon(t)\, dt < 1$ within the studying temporal scale, the fraction of the left inertia vorticity after dissipation. Under the boundary conditions $U(x=0)=U_w$, $U(x=x_e)=Ue$, and $1/x_e^{-2} << 1$, the solution of Eq. 21 is, according to Jr. Malley [9].

$$U = \frac{H}{H_o}U_e + \frac{H}{S_x R_e}\{\sum_{i=M}^{S}\frac{g_{io}}{f_e}[A_{ix} + B_{iH} - B_{iH_o}] + 2f_e C_k cos\varphi(x_e - x)\} \quad (22)$$

where

$$A_{ix} = C_i(3 + cos2\varphi)sinb\cos(t_f + b) + \frac{1}{4}cos\varphi^2 sin2b\cos(2t_f + 2b) \quad (23)$$

$$B_{iH} = \sin(t_f + a_H)[C_i + \frac{1}{8}\cos(t_f + a_H)] - a_H[C_i\cos(t_f + a_H) + \frac{1}{8}\cos(2t_f + 2a_H) + C_i q_{1H}] + \frac{1}{4a_H}q_{2H} \quad (24)$$

$$B_{iHo} = \sin(t_f + a_{Ho})[C_i + \frac{1}{8}\cos(t_f + a_{Ho})] - a_{Ho}[C_i\cos(t_f + a_{Ho}) + \frac{1}{8}\cos(2t_f + 2a_{Ho}) + C_i q_{1Ho}] + \frac{1}{4a_{Ho}}q_{2Ho} \quad (25)$$

$$q_{nHo} = a_{Ho}\sin(nt_f)\,CosInt(na_{Ho}) + a_{Ho}\cos(nt_f)\,SinInt(na_{Ho}) \quad (26)$$

(n=1 or 2)

$$a_{Ho} = \frac{H_o}{S_x R_e cos\varphi} \quad (27)$$

$$b = \frac{x_e - x}{2R_e cos\varphi} \quad (28)$$

Influence of the shelf on the shelf current

Without the shelf slope, the amplitude of the SMG-induced current can be estimated as

$$U \sim \sum_{i=M}^{S}\frac{g_{io}}{f_e} \quad (29)$$

With the shelf slope, the amplitude of the SMG-induced current can be estimated as

$$U \sim \frac{H}{S_x R_e}\sum_{i=M}^{S}\frac{g_{io}}{f_e} \quad (30)$$

Compare Eq. 29 and Eq. 30, the approximate amplifying coefficient for shelf currents due to the shelf slope can be estimated as

$$A_m = \frac{H}{S_x R_e} \quad (31)$$

Related to the Earth's radius, the thicker and/or the slower slope, the stronger are the shelf current induced by the SMG and by inertial motion if $Am > 1$ within zonal zones of 6°N – 10°N and 2°S – 2°N of the west shelf of the Pacific Ocean. The amplifying coefficients of the western shelves of the oceans are listed in Table 1 below.

Table 1: Amplifying coefficients of the western shelves of the oceans

Zonal Zone	Indian	Pacific	Atlantic
6°N – 10°N	0.135	1.425	0.212
2°S – 2°N	0.183	1.383	0.194
6°S – 10°S	0.125	0.762	0.114

There is a big difference in the amplifying coefficients among the western shelves of the Indian, Pacific, and Atlantic Oceans. The large and slow western shelf of the Pacific Ocean maintains or intensifies the flow on it, while the small and sharp western shelves of the Indian and Atlantic oceans reduce the flow on it (Fig.3 and Fig.4).

With the east boundary current of -10 mmS^{-1}, the west shelf of the Pacific within zonal zones of 6°N − 10°N and 2°S − 2°N intensifies the east boundary current into -15 mmS-1 near the bottom of the ocean and then the flow reduces to zero as the water depth gets shallower, while the west shelves of the Indian and Atlantic Oceans reduce the east boundary flow to zero with the water depth gets shallower (Fig.3).

Without the east boundary flow, the west shelf of the Pacific within zonal zones of 6°N − 10°N and 2°S − 2°N still produces a significant current and a large flux, up to 7×10^6 m^3S^{-1} at a section of 2000 meter depth and 4 degree zonal width, while the west shelves of the Indian and Atlantic Ocean only produce a very weak flow (Fig.4).

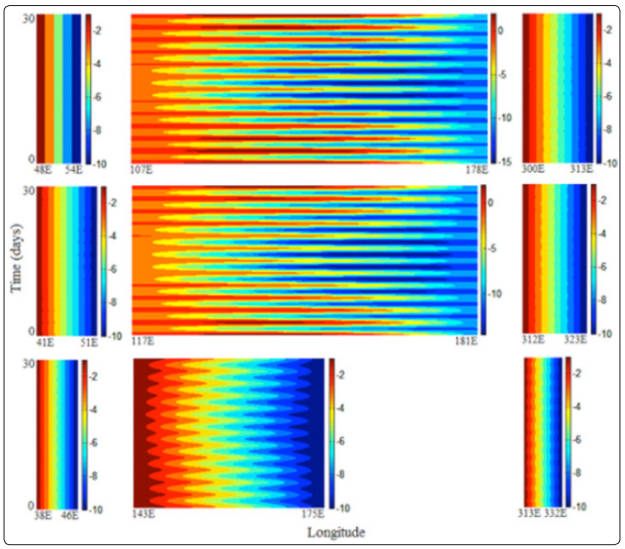

Figure 3: SMG-induced currents (mmS^{-1}) on the western selves of the Indian (column 1), Pacific (column 2), and Atlantic (column 3) within zonal belts of 6°N − 10°N (row 1), 2°S − 2°N (row 2), and 6°S − 10°S (row 3). U_e is set as 10 mmS^{-1}.

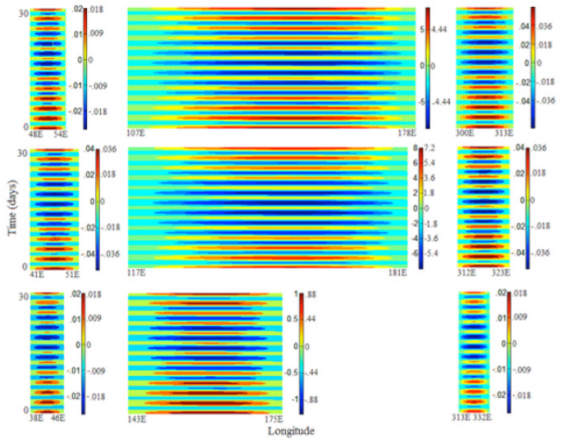

Figure 4: SMG-induced currents (mmS^{-1}, scales on the left hands of the color bars) and their flux at a cross-section of 2000m depth and 4-degree latitude ($\times10^6 m^3S^{-1}$, scales on the right hands of the color bars) on the western selves of the Indian (column 1), Pacific (column 2), and Atlantic (column 3) within zonal belts of 6°N − 10°N (row 1), 2°S − 2°N (row 2), and 6oS − 10oS (row 3). U_e is set as 0 mmS^{-1}.

Discussions

The SMG can be the major vorticity source for the entire depth of water column within tropical oceans, approximately 2 to 4 times of that provided by wind stress. Related to the Earth's radius (Re), thickness (H) of water column, and shelf's slope (S_x), the SMG-induced shelf currents can be amplified by $HS_x^{-1} R_e^{-1}$ times due to the shelf's slope. The large and slow west shelf of the Pacific Ocean intensifies the flows on it within zonal zone of approximately 2°S − 10°N where the Kuroshio is located, much more than the small and sharp west shelves of the Indian and Atlantic Oceans. The characteristics of the SMG waves and the ocean geometry may help explain the fact that the ENSO oscillation is more prominent in the Pacific Ocean than in the Atlantic and Indian Oceans.

References

1. Kelly KA, Gille ST (1990) Gulf Stream surface transport and statistics at 69W from the GEOSAT altimeter. J. Geophys. Res 95: 3149-3161.
2. Qiu B (2000) Interannual variability of the Kuroshio Extension system and its impact on the wintertime SST field. J. Phys. Oceanogr 30: 1486-1502.
3. Qiu B (2003) Kuroshio extension variability and forcing of the Pacific decadal oscillations: Responses and potential feedback. J. Phys. Oceanogr 33: 2645-2482.
4. Kelly KA, Dong S (2004) The relationship of western boundary current heat transport and storage to mid-latitude ocean-atmosphere interaction. Earth's Climate: The Ocean Atmosphere Interaction, S.-P. X. C. Wang and J. A. Carton, Eds., American Geophysical Union Geophysical Monograph 147: 347-363.
5. Qiu B, Chen S (2005) Variability of the kuroshio extension jet, recirculation gyre, and mesoscale eddies on decadal time scales. J. Phys. Oceanogr 35: 2090-2103.
6. Minobe S, Kuwano-Yoshida A, Komori N, Xie SP, Small RJ (2008) Influence of the Gulf Stream on the troposphere. Letters to Nature 452: 206-209.
7. Kelly KA, Small RJ, Samelson RM, Qiu B, Joyce TM et al. (2010) Western Boundary Currents and Frontal Air–Sea Interaction: Gulf Stream and Kuroshio Extension. J. of Climate 23: 5644-5667.
8. Wang Z (2016) Preliminary studies of climate-environment dynamics for our Climate Prediction and Environment, Outskirt Press, ISBN 9781478779032, p 308.
9. Malley REO Jr (1991) Singular Perturbation Methods for Ordinary Differential Equations. Applied Mathematical Sciences, 89, pp225, Springer Verlag.